Proceedings of 2022 IEEE
International Conference on Mechatronics and Automation
August 7 - 10, Guilin, China

The Terrestrial Gait Design of the Bionic Robotic Duck

Zhengyu Li[1], Liwei Shi[1]*, Shuxiang Guo[1,]*, Zhongyin Zhang[1], Meng Liu[1], Bao Pengxiao[1]

[1]*Key Laboratory of Convergence Medical Engineering System and Healthcare Technology, the Ministry of Industry and Information Technology, School of Life Science, Beijing Institute of Technology, No.5, Zhongguancun South Street, Haidian District, Beijing 100081, China*

E-mails: lizhengyu@bit.edu.cn; shiliwei@bit.edu.cn; guoshuxiang@bit.edu.cn; zhangzhongyin@bit.edu.cn

* Corresponding author

***Abstract* - With the increasing demand for ocean exploration, amphibious robots can integrate the advantages of underwater and land robots, and can achieve detection on land, underwater, and seabed. Underwater robots or land robots generally can only work in a single environment, but amphibious robots can adapt to complex and diverse environments, such as completing the dredging work of small and medium-sized rivers, lakes, wetlands, and swamps, and it could also be used for coastline patrol in military. This topic proposed the idea of bionic waterfowl, designed a set of amphibious bionic waterfowl robot prototype, and built the machinery platform and control system platform. The robot's dynamic leg and head and neck are moved by modeling; the land gait design and simulation analysis of the robot are carried out by ADAMS software. Through the analysis of the simulated gait, it is determined that the gait is stable and efficient, which lays the foundation for the actual control of the subsequent prototype.**

Index Terms - Structural design. Kinematics modeling. The gait designs.

I. Introduction

At present, bionic amphibious robots are attracting a lot of publicity from military and commercial sector because of their high-performance capabilities both underwater and on land [1-3]. And for bionic amphibious robots, there are multiple sports modes both underwater and on land to meet the needs of different environments. The bionic amphibious robot draws on the movement mechanism and movement ability of amphibians, so that the robot can drive normally on land and underwater. Moreover, they also have some advantages of efficient obstacle avoidance, strong maneuverability, and fast transition between land and water [4-7].

In recent years, research on bionic underwater vehicles developed gradually.

Xing *et al*. designed a miniature bio-inspired Amphibious Spherical Robot (ASRobot) with a Legged, Multi-vectored Water-jet Composite Driving Mechanism (LMWCDM). They studied locomotory performance of the robot in amphibious field environments. And the results demonstrate that the robot prototype possesses the high locomotory performance [8].

Guo *et al*. proposed a decentralized method of spherical amphibious multi-robot control system based on blockchain technology. They set up the point-to-point information network based on long range radio technology of low power wide area network, and designed the blockchain system for embedded application environment and the decentralized hardware and software architecture of multi-robot control system. On this basis, the consensus plugin, smart contract and decentralized multi-robot control algorithm were designed to achieve decentralization. The experimental results of consensus of spherical amphibious multi-robot showed the effectiveness of the decentralization [9].

Zheng *et al*. design an artificial multi-robot cooperative mode and explore an electronic communication and collaborate devices, the control method is based in particular on underwater environment and also conduct a detailed analysis of control motion module [10].

Shi *et al*. used a fuzzy Proportional-Integral-Derivative (PID) control algorithm to design an underwater motion control system for a novel robot. Moreover, they compared PID with fuzzy PID control methods by carrying out experiments on heading and turning bow motions to verify that the fuzzy PID is more robust and exhibits good dynamic performance. They also carried out experiments on the three-dimensional (3D) motion control to validate the design of the underwater motion control system [11].

Shi *et al*. developed a small-sized quadruped robotic rat (SQuRo), which includes four limbs and one flexible spine, They proposed a control framework for multimodal motion planning, and the appropriate control parameters were tuned through optimization with consideration to the stability and actuation limits. The results obtained through a series of experimental tests reveal that SQuRo achieves a superior motion performance compared with existing state-of-the-art small-sized quadruped robots [12].

Shi *et al*. proposed key movement joints (KMJs) to capture a decent representation of the rat with a reduced-order model. By extracting the primary KMJs, they determined the number and distribution of robotic joints for the design of a bioinspired spine mechanism. To meet the demand of high biomimicry degree, they generated an optimal compensation term to minimize the trajectory error introduced by simplifying the model. And they calculated the optimal minimum motion cycle based on the constraints of equilibrium under extreme conditions to ensure high flexibility without compromising the stability. The proposed method was successfully verified through simulation and experimental tests with a robotic rat end Researchers have designed bionic robots by studying crabs, lobsters, turtles, snakes, frogs and other amphibians in nature and imitating their driving mechanisms in different environments [14-18]. The world's first bionic amphibious robot was an autonomous crab-like robot called Ursula that was designed for mine hunting in the surf zone in 1996[15]. A large number of bionic amphibious robots that are based on lobsters, turtles, snakes, and other creatures emerged one after another [14,19-21].

The driving mechanism of underwater and terrestrial creatures is an important part of bionic amphibious robots. There are two main ways to drive traditional underwater robots： propeller and water jet driving. However, these two methods have the disadvantages of low efficiency, poor biological affinity, and great environmental damage [22]. Aquatic organisms have gradually evolved a variety of movement patterns in order to adapt to different underwater environments. Traditional non-bionic land driving mainly includes the wheel driving mode and track driving mode, which are widely used in industry. Traditional non-bionic land driving mainly includes the wheel driving mode and track driving mode, which are widely used in industry. However, the motion is not smooth on the complex road surface near the coast and the ideal motion performance cannot be developed. In nature, some organisms that have been selected for a long time can move freely on land or in water, with superior propulsion performance. Due to its stronger environmental adaptability and obstacle surmounting ability, bionic driving modes have attracted the attention of research institutions around the world over the past few decades. According to their motion forms, they can be divided into legged walking, legged jumping, and limbless locomotion [23-26].

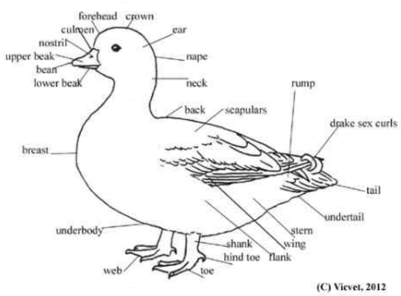

Fig. 1 Duck body structure [27]

When walking on land, many ducks have to stand upright to balance the center of gravity before and after due to the hindmost of their legs, but they still swing from side to side when walking. Even some ducks have to support their bodies with their wings to crawl forward on land because the hindmost of their legs are too close to the tail by studying and observing the physiological structure and movement characteristics of ducks, we can determine the structure of the robot and the movement mode of each joint, to complete the basic research on the structure bionics and movement bionics of the bionic waterfowl robot.

In this paper, a bionic amphibious robot is proposed, and its mechanical system is designed, which is divided into head, body, and legs. The kinematics of the legs are analysed. Based on this, a stable and feasible land gait is designed. The simulation of Adams will help to realize the actual control of the robot prototype in the next step.

The rest of this paper is organized as follows. Section II introduces the mechanical structure of the robot and kinetics analysis of leg. In Section III, the terrestrial gait analysis, simulation and result are detailed. Finally, the conclusion is summarized in Section IV.

II. Structure And Analysis

After observing the waterfowl, we have an understanding of its biological shape, body structure, movement mode, and other aspects. To realize the bionic waterfowl robot walking on land and swimming in the water, the mechanical mechanism of the robot is designed, and the overall structure of the robot is divided into the head, neck, and leg waterproof shell and other parts.

A. Mechanical structure design

1) Head: The parameters of each joint are shown in Table I.

TABLE I
BIONIC WATERFOWL HEAD AND NECK PARAMETERS

Part	Length (mm)	Movement direction	Angle range
Base section	130	Horizontal	-90~90°
Middle section	50	Vertical	-90~90°
Nearly head-end	100	Vertical	-90~90°
Head	85	Vertical	-180~180°

2) Legs： The legs of the bionic waterfowl robot are mainly divided into dynamic legs and soles and auxiliary legs three parts.

The overall structure of the duck is in Fig. 2.

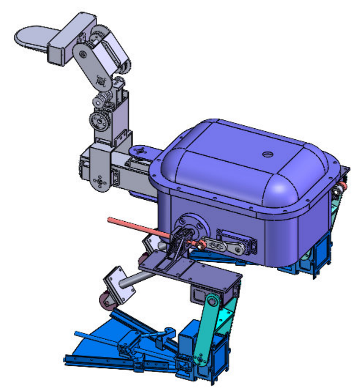

Fig. 2 Overall structure of the duck

B. Define the coordinate system

The mechanical structure of the amphibious bionic waterfowl robot studied in this paper has been introduced in detail in the previous chapter, according to the joint sites of this model, as shown in Fig. 3.

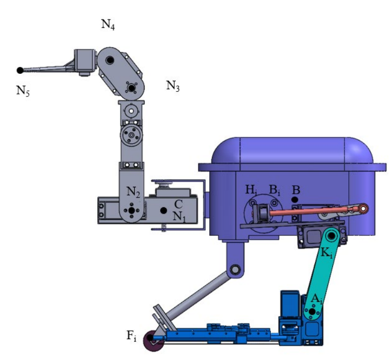

Fig. 3 Joint sites of amphibious bionic waterfowl robot

C. *Kinetics Analysis of Leg*

The model analysis of the left leg of the robot is carried out. ${}^{O}_{F1}P$ and ${}^{O}_{B}P$ are the position vectors of the left leg foot end $F1$ and the robot center of mass B in the global coordinate system {O} respectively, and θ_{11}, θ_{12} and θ_{13} are the joint variables respectively.

1) Robot Support Leg Analysis: Firstly, the forward kinematics analysis of the robot's supporting legs is carried out, and the pose ${}^{O}_{B}P$ and ${}^{O}_{B}R$ of the robot are solved immediately through ${}^{O}_{F1}P$ and θ_{11}, θ_{12} and θ_{13}.

$$ {}^{F_1}_{B_1}T=A_1A_2A_3A_4=\begin{bmatrix} {}^{F_1}_{B_1}R & {}^{F_1}_{B_1}P \\ 0 & 1 \end{bmatrix}= \begin{bmatrix} C_{11+12+13} & 0 & S_{11+12+13} & l_1S_{12+13}+l_2S_{13} \\ 0 & 1 & 0 & 0 \\ -S_{11+12+13} & 0 & C_{11+12+13} & l_1C_{12+13}+l_2C_{13}+l_3 \\ 0 & 0 & 0 & 1 \end{bmatrix} \quad (1) $$

In the formula, S_{i+j} Express $sin(\theta_i+\theta_j)$, C_{i+j} Express $cos(\theta_i+\theta_j)$, i, j= 11,12,13.

2) Robot swing leg analysis: If the pose of the robot's center of mass and the variables of each joint are known, the swinging leg of the robot can be analysed to obtain the pose of the foot end F_1 of the swinging leg.

$$ {}^{F_1}_{B_1}T=A_1'A_2'A_3'A_4'= \begin{bmatrix} C_{11+12+13} & 0 & -S_{11+12+13} & l_3S_{11+12+13}+l_2S_{11+12}+l_1S_{11} \\ 0 & 1 & 0 & 0 \\ S_{11+12+13} & 0 & C_{11+12+13} & -l_3C_{11+12+13}-l_2C_{11+12}-l_1C_{11} \\ 0 & 0 & 0 & 1 \end{bmatrix} \quad (2) $$

The power leg is composed of a crank-rocker structure and a two-link structure, as shown in Fig. 4, which can provide three degrees of the freedom movement in the vertical plane. The robot hip joint is a crank rocker structure, which can provide periodic swings for the entire leg. The advantage of this design is that the motor only needs to keep rotating to produce the swing effect, which avoids the damage to the motor caused by the directly repeated swing of the motor. The knee joint and ankle joint form a two-link structure, which provides more swing space for the sole of the foot.

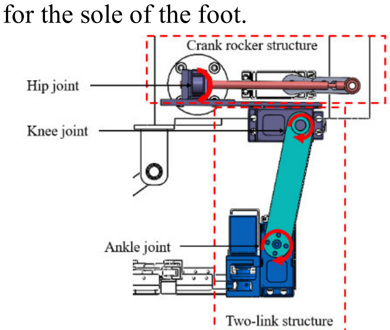

Fig. 4 Power Leg Structure

3) Robot head and neck analysis: The head and neck of waterfowl are relatively slender and have many bones and joints, thus providing convenience for predation and observation. From the perspective of robot application, the multi-degree-of-freedom design undoubtedly brings a wider field of vision and provides great convenience in robot positioning and target recognition. But from the design point of view, the multi-joint design takes up too much space and is difficult to control. Therefore, in general, to meet the vision and facilitate control, the bionic waterfowl robot has designed a three-degree-of-freedom head and neck structure.

$$ {}^{C}_{N_5}T=S_1S_2S_3S_4S_5= \begin{bmatrix} C_{5+6+7} & 0 & -S_{5+6+7} & l_7S_{5+6+7}+l_6S_{5+6}+l_5S_5 \\ S_4S_{5+6+7} & C_4 & S_4C_{5+6+7} & -S_4(l_7S_{5+6+7}+l_6S_{5+6}+l_5C_5+l_4) \\ C_4S_{5+6+7} & -S_4 & C_4C_{5+6+7} & -C_4(l_7S_{5+6+7}+l_6S_{5+6}+l_5C_5+l_4) \\ 0 & 0 & 0 & 1 \end{bmatrix} \quad (3) $$

III. Terrestrial Gait Analysis

A. *Adams Model Building*

The specific process of establishing the virtual prototype model in ADAMS is as follows:

1) Import the 3D model of the robot in Parasolid (.x_t) format;

2) Set basic information such as the name, material, or quality of the part;

3) Create a joint between components

4) Apply a drive (Motion) to the motion-related joints;

5) Establish the contact model between the foot and the ground.

A total of 12 rotation pairs and 2 translation pairs are established for the head, legs, and auxiliary legs. To realize the robot motion, the rotation driving function is added to the 6 joints of the leg, and the other joints do not add rotation. Auxiliary legs and soles of the robot are the components that are in contact with the ground, and collision constraints are set. At the same time, the friction force of the contact is set, so that the robot can obtain a forward driving force during the simulation to complete the normal walking of the robot.

The virtual prototype model of the amphibious bionic waterfowl robot is shown in Fig. 5.

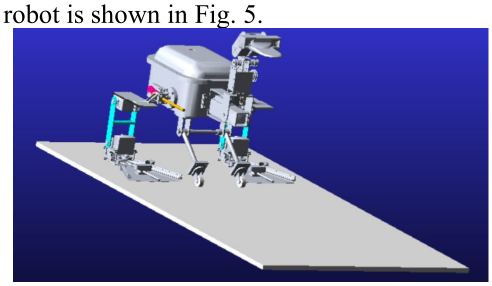

Fig. 5 Robot virtual prototype model

B. *Terrestrial Gait Analysis*

The rational design of the robot's gait on land is an important step to realize the simulation. Here, it is necessary to comprehensively consider the robot structure and make reasonable use of the motion space, to complete a relatively stable walking. After the gait design, it is necessary to analyze the various joints that complete the gait, to provide an important theoretical reference for the final realization of the prototype motion.

To realize the robot's land walking, this study designed the robot's land gait. Take the robot's initial gait posture as the right foot is raised and the left foot is on the ground as an example, as shown in Fig. 6, The robot initially stands on the ground, with a 180° phase difference between the left and right hip joints.

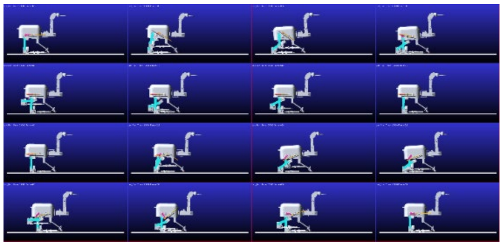

Fig. 6 Overland Gait Chart

The hip joint of the right leg swings upward clockwise to lift the following joints; The left hip joint swings down a certain angle clockwise, and the knee joint below it cooperates with the ankle joint. The sole of the foot pushes forward by using the ground friction. At this time, the robot takes a step forward. After that, the left leg remains at the same angle and is supported on the ground until the right hip drives the rod swings back to the horizontal position again, the robot's lower leg is vertical and the sole of the foot stands on the ground. The right leg supports the ground and does not move. The left leg uses the remaining space to retract the leg until the driving rod of the left leg turns to the horizontal position. At this time, the state of the robot is symmetrical with the initial state. The right foot pushes on the ground and the left leg raises. At this time, the robot takes another step forward. Keep the right leg supporting the ground and wait for the left leg to continue to rotate 180 ° before landing. The left leg supports the ground and does not move. The right leg uses the remaining space to retract the leg until the driving rod of the right leg turns to the horizontal position. At this time, the state of the robot is the same as the initial state, to complete the starting and one cycle gait. As shown in Fig. 8, it is the schematic diagram of the rotation of the robot's hip joint, knee joint, and ankle joint. The dark strip part indicates that the current leg is in contact with the ground. L represents the left leg and R represents the right leg. The degree represents the angle at which the hip crank rotates at this time. The robot is driven by the STEP function of ADAMS software, which controls the rotation of the hip joint, knee joint, and ankle joint step by step, and the motion of the whole cycle is superimposed.

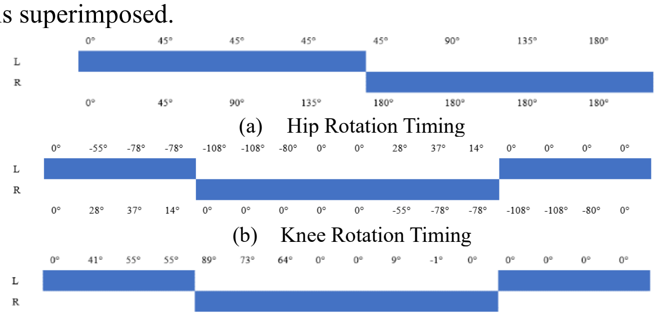

(a) Hip Rotation Timing

(b) Knee Rotation Timing

(c) Ankle Rotation Timing

Fig. 7 Joint rotation timing

C. Experiment Analysis

In Adams's environment, according to the gait of the robot, each cycle takes 4S to design, and the simulation runs for 12s. A total of three cycles of motion are carried out. Obtain the kinematics and dynamics data of the robot through the monitoring module; In the post-processing module, the simulation results of the graphical robot according to the gait, including the centroid displacement and speed of the robot body, the robot step size, the driving torque, rotation angle and angular speed of each joint.

As shown in Fig. 8, the robot is propelled intermittently. Fig. 8 (a) shows the displacement track of the robot body centroid along the moving direction, and Fig. 8 (b) shows the fluctuation of the robot body centroid in the vertical direction. The vibration range is within 15mm and the robot is propelled.

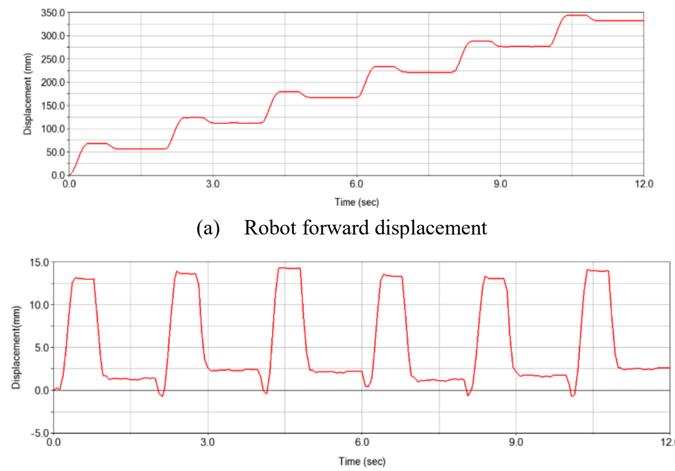

(a) Robot forward displacement

(b) Robot vertical displacement

Fig. 8 Robot body displacement

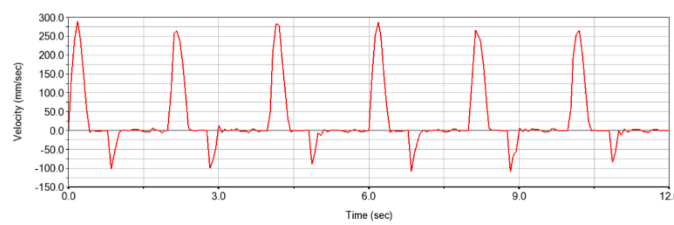

Fig.9 Robot body speed

As shown in Fig.10, it is the instantaneous velocity trajectory of the robot centroid, and the slope of the curve represents the acceleration of the robot. It can be seen that in the motion cycle of the robot, the inertia of the leg swing has a slight impact on the body, and the impact is small when the ground static friction is large.

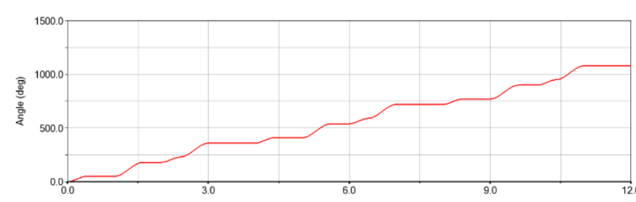

(a) Crank rotation angle of robot hip joint

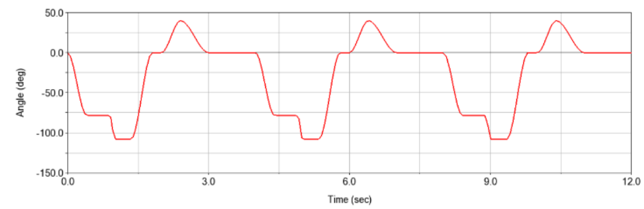

(b) Robot knee rotation angle

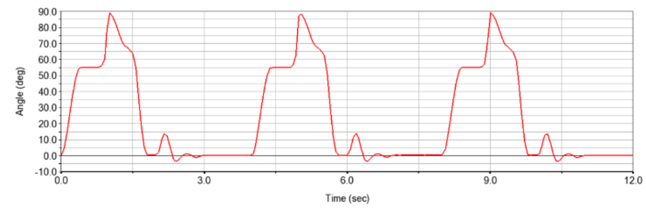

(c) Rotation angle of robot ankle

Fig. 10 rotation angle of robot joint

As shown in Fig.10, the rotation angle trajectories of the left hip crank, knee, and ankle of the robot during walking are shown respectively. The joint rotation is generated by the software built-in function STEP (time, x_0, h_0, x_1, h_1). Where, time is an independent variable, indicating time; x_0 represents the start value of the period, and x_1 represents the end value of the period; h_0 represents the start value of joint rotation angle in this period, and h_1 represents the end value of joint rotation angle in this period. The realization of this function can provide a reference for the motor control of the prototype.

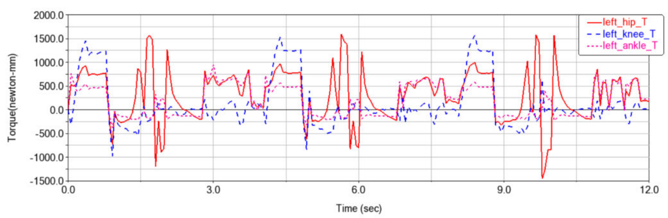

Fig.11 Robot joint torque

As shown in Fig.11, it is the joint torque of the robot's hip crank, knee, and ankle during walking. Because the hip joint drives the knee joint and ankle joint, the driving torque of the hip joint is slightly greater than that of other joints. The driving torque of the knee joint is also slightly larger than that of the ankle joint. Therefore, the above analysis is consistent with the simulation results. Some peaks with large changes in the figure are caused by the instability of the robot due to the contact between the legs and the ground. Because the robot prototype mainly moves through the driving force on the joint, the size of the driving torque is very important for the selection of the motor on the joint of the prototype. The selected motor shall meet the torque required in the simulation. The maximum driving torque is 33kgf.cm, the maximum driving torque required for the knee joint is 16kgf.cm, and the maximum driving torque required for the knee joint is 11kgf.cm, which provides a certain reference for motor selection.

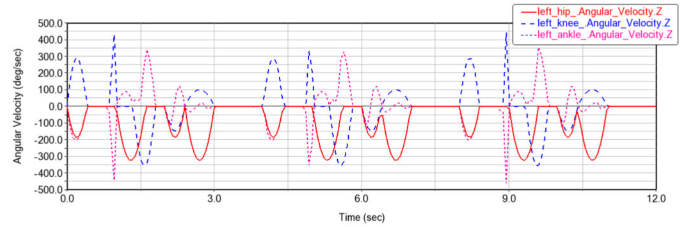

Fig.12 Angular velocity of robot joint

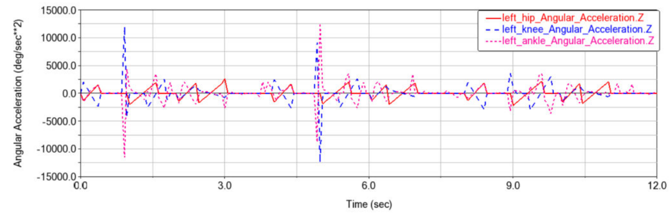

Fig.13 Angular acceleration of robot joint

The angular velocity and angular acceleration of robot joints are important parameters to reflect the motion of the robot. Next, the changes of angular velocity and angular acceleration in the motion of the robot are analysed. As shown in Fig.12 and 13, the left leg of the robot. It can be seen that each measurement quantity changes periodically, and it provides a reference for the accuracy of the control. Each time the robot's hip crank drives its lower leg component to lift, the angular velocity of each joint will change greatly. There are some differences due to the contact and collision between the support leg and the ground.

This section analyses the land gait of the bionic duck through Adams, the simulation results show that the robot can complete forward propulsion and the center of mass can remain stable, so the gait design is reasonable. Besides, the simulation analysis of torque and angular velocity provides help in selecting motors and optimizing robots.

IV. RESULT

In this study, the design of a bionic duck robot is proposed. The proposed mechanical design includes head and neck design, leg design, and waterproof shell design. At the same time, the design of the land gait of the bionic duck robot is realized, the virtual prototype development software is used to realize the simulation of the robot's land gait, and monitor the parameters of the robot body, swing legs, and various joints in motion, to provide important guidance for the robot's motor selection and motor control.

However, limited by the research time, only the land gait simulation has been achieved. In the future, the underwater gait simulation and the actual control of underwater and land motion experiments will be carried out. At the same time, the land and underwater gait are further optimized. By comparing the speeds of different gaits, we can explore a more reasonable gait that is more in line with the bionic effect. In addition, the robot can combine a variety of sensor settings and adopt a variety of control methods. For example, the CPG control method is applied to the leg swing action, to make the robot gait closer to biological motion, have better motion performance, and be more practical.

ACKNOWLEDGEMENT

This work was supported by National Natural Science Foundation of China (61773064, 61503028).

REFERENCES

[1] E. Milana et al., "EELWORM: a bioinspired multimodal amphibious soft robot," *2020 3rd IEEE International Conference on Soft Robotics (RoboSoft)*, pp. 766-771, 2020.

[2] H. Xing et al., "A Novel Small-scale Turtle-inspired Amphibious Spherical Robot," *2019 IEEE/RSJ International Conference on Intelligent Robots and Systems (IROS)*, pp. 1702-1707, 2019.

[3] T. Paschal, M. A. Bell, J. Sperry, S. Sieniewicz, R. J. Wood and J. C. Weaver, "Design, Fabrication, and Characterization of an Untethered Amphibious Sea Urchin-Inspired Robot," in *IEEE Robotics and Automation Letters*, Vol. 4, no. 4, pp. 3348-3354, Oct. 2019.

[4] B. Zhong, S. Zhang, M. Xu, Y. Zhou, T. Fang and W. Li, "On a CPG-Based Hexapod Robot: AmphiHex-II With Variable Stiffness Legs," in *IEEE/ASME Transactions on Mechatronics*, Vol. 23, no. 2, pp. 542-551, April 2018.

[5] Graf, N.M., Behr, A.M., Daltorio, K.A. "Crab-Like Hexapod Feet for Amphibious Walking in Sand and Waves," In: et al. *Biomimetic and Biohybrid Systems. Living Machines 2019. Lecture Notes in Computer Science()*, Vol 11556. Springer, Cham., 2019.

[6] T. Tanaka, H. Sakai and J. Akizono, "Design concept of a prototype amphibious walking robot for automated shore line survey work," *Oceans '04 MTS/IEEE Techno-Ocean '04 (IEEE Cat. No.04CH37600)*, Vol. 2, pp. 834-839, 2004.

[7] Sequeira A A, Usman A, Tharakan O P, et al. "Biologically Inspired Robots into a New Dimension-A Review". *International Journal of Automation, Mechatronics & Robotics*, Vol. 3, no. 1, pp. 106-116, 2016.

[8] H. Xing, L. Shi, X. Hou, Y. Liu, Y. Hu, D. Xia, Z. Li, S. Guo. "Design, Modeling and Control of a Miniature Bio-inspired Amphibious Spherical Robot", *Mechatronics*, Vol. 77, No. 1, 2021.

[9] S. Guo, S. Cao, J. Guo. "Study on Decentralization of Spherical Amphibious Multi-robot Control System Based on Smart Contract and Blockchain", *Journal of Bionic Engineering*, 2021.

[10] L. Zheng, S. Guo, Y. Piao, S. Gu, R. An. "Collaboration and Task planning of Turtle-Inspired Multiple Amphibious Spherical Robots" *Micromachines*, 2020.

[11] L. Shi, Y. Hu, S. Su, S. Guo, H. Xing, X. Hou, Y. Liu, Z. Chen, Z. Li, D. Xia. "A Fuzzy PID Algorithm for a Novel Miniature Spherical Robots with Three-dimensional Underwater Motion Control", *Journal of Bionic Engineering*, pp. 1-11, 2020.

[12] Qing Shi, Junhui Gao, Shengjie Wang, Xiaolong Quan, Guanglu Jia, Qiang Huang, Toshio Fukuda. "Deveopment of a Small-Sized Quadruped Robotic Rat Capable of Multimodal Motions." *IEEE Transactions on Robotics*, 2022. DOI: 10.1109/TRO.2022.3159188

[13] Qing Shi, Zihang Gao, Guanglu Jia, Chang Li, Qiang Huang, Hiroyuki Ishii, Atsuo Takanishi, Toshio Fukuda. "Implementing Rat-Like Motion for a Small-Sized Biomimetic Robot Based on Extraction of Key Movement Joints." *IEEE Transactions on Robotics,* vol. 37, no. 3, pp. 747-762, 2021.

[14] G. Dudek et al., "AQUA: An Amphibious Autonomous Robot," in *Computer*, Vol. 40, no. 1, pp. 46-53, Jan. 2007.

[15] H. Greiner, A. Shectman, Chikyung Won, R. Elsley and P. Beith, "Autonomous legged underwater vehicles for near land warfare," *Proceedings of Symposium on Autonomous Underwater Vehicle Technology*, pp. 41-48, 1996.

[16] Dowling, Kevin J. "Limbless locomotion: learning to crawl with a snake robot," *Carnegie Mellon University*, 1997.

[17] Han, Bin, et al. "Mechanism design and gait experiment of an amphibian robotic turtle." *Advanced Robotics* vol. 25, no. 16 pp. 2083-2097, 2011.

[18] Y. Tang, L. Qin, X. Li, C. -M. Chew and J. Zhu, "A frog-inspired swimming robot based on dielectric elastomer actuators," *2017 IEEE/RSJ International Conference on Intelligent Robots and Systems (IROS)*, pp. 2403-2408, 2017.

[19] Ayers, Joseph, et al. "Lobster robots." (2000).

[20] Kemp, Mathieu, Brett Hobson, and John H. Long. "Madeleine: an agile AUV propelled by flexible fins." *Proceedings of the 14th International Symposium on Unmanned Untethered Submersible Technology*. Vol. 6. USA, 2005.

[21] P. Liljebäck, Ø. Stavdahl, K. Y. Pettersen and J. T. Gravdahl, "Mamba - A waterproof snake robot with tactile sensing," *2014 IEEE/RSJ International Conference on Intelligent Robots and Systems*, pp. 294-301, 2014.

[22] A. Carof, "Miniaturized and reconfigurable instrumentation for multipurpose survey with a Mini Autonomous Underwater Vehicle MAUVE-project," *Proceedings of Symposium on Autonomous Underwater Vehicle Technology,* pp. 28-32, 1996.

[23] Grzelczyk, Dariusz, and Jan Awrejcewicz. "Modeling and control of an eight-legged walking robot driven by different gait generators." *International Journal of Structural Stability and Dynamics,* vol. 19, no. 5, pp. 1941009, 2019.

[24] Zhang, Chi, et al. "Biologically inspired jumping robots: A comprehensive review." *Robotics and Autonomous Systems,* vol.124, pp. 103362,2020.

[25] Ding, Yang, et al. "Emergence of the advancing neuromechanical phase in a resistive force dominated medium." *Proceedings of the National Academy of Sciences,* vol. 110, no. 25, pp. 10123-10128, 2013.

[26] Roy, Shibendu Shekhar, and Dilip Kumar Pratihar. "Multi-body Dynamic Modeling of Multi-legged Robots," *Springer Nature*.

[27] V. Roberts, VICVET, January 2012. Accessed on: April 9, 2022. Available: https://vicvet.com/otherpoultry.php.